Heliyon 5 (2019) e02706

Contents lists available at ScienceDirect

Heliyon

journal homepage: www.heliyon.com

Research article

Effect of through thickness separation of fiber orientation on low velocity impact response of thin composite laminates

Ankush P. Sharma [a,*], Sanan H. Khan [b], R. Velmurugan [a]

[a] Department of Aerospace Engineering, Indian Institute of Technology Madras, Chennai, India, 600036
[b] Department of Mechanical Engineering, Aligarh Muslim University, Aligarh, India, 202002

ARTICLE INFO

Keywords:
Materials science
Mechanical engineering
Composites
Low velocity impact
Delamination
Energy absorbed
Structural analysis
Composite materials
Materials characterization
Mechanical property
Structural behavior

ABSTRACT

The effect of separation of fiber orientation through the thickness of thin composites on their low velocity impact response is studied. The composites are prepared using unidirectional glass fiber reinforced epoxy through hand layup followed by vacuum bagging. The two dissimilar layups of composites considered have separation of composite layers with fibers having the same and different orientations through the thickness. The composites are subjected to low velocity impact using a drop-weight testing machine. The composites are evaluated using different performance parameters such as damage degree, first damage and maximum forces, first cracking energy, bending stiffness, elastic strain energy, elastic, residual and maximum displacements, permanent deformation, square-root delaminated area, delamination length and width, and contact duration. Among the two composites, it is observed that [90/-45/45/0] composite in which two layers with fibers having 90° and 0° orientations separating by two layers with fibers having -45° and 45° orientations, levels of deformation are lower and recorded force and square-root delaminated area are higher and lower, respectively for the same level of impact energy. Whereas, in case of [0/90/90/0] composite in which two layers with fibers having 0° orientations separating by two layers with fibers having 90° orientations, recorded force is lower and deformation and square-root delaminated area are higher. The [0/90/90/0] composite is having a comparatively more lateral spread of delamination and inter-layer opening than that of [90/-45/45/0] composite considering extensional and bending stiffnesses along longitudinal (A_{11}, D_{11}) and transverse (A_{22}, D_{22}) directions. This facilitates that lateral spread of damage within composite can be decreased by separating two layers of composite with 90° and 0° fiber orientations by two layers with -45° and 45° fiber orientations, i.e., [90/-45/45/0] composite.

1. Introduction

The need for materials with a high stiffness-to-weight ratio and the high strength-to-weight ratio has led to the rise of composites [1]. Composite materials have a lower density, higher stiffness, higher strength, and better fatigue resistance compared to traditional metallic materials such as steel or aluminum [2]. Aircraft, tanks, bullet-proof body armors, etc. are made of advanced composites. Aerospace structures, automotive industry, and transportation sector make use of composites [3]. The performance of many advanced engineering structures and components undergoing impact significantly depend upon the corresponding behavior of composites [4, 5, 6]. During service life, the response of composites on their low velocity impact behavior should be clearly understood, for instance, dropping the tool onto a composite during maintenance or effect of a flying fragment. The work has been carried out by various researchers contributing to the suitable understanding and enhancing the behavior of fiber reinforced plastic (FRP) laminates on impact.

Choi et al. [7] have observed that for graphite/epoxy laminates, change of stacking sequence significantly influences impact damage much more than the change of thickness. Kessler and Bledzki [8] have investigated that cross-ply laminated composite plates with poor adhesion are poor damage resistant than laminates with good fiber/matrix adhesion. Schoeppner and Abrate [9] have investigated that graphite/BMI laminates are having higher delamination threshold load (DTL) and damage resistance over the entire range of laminate thicknesses compared to graphite/epoxy and graphite/PEEK laminates when subjected to low velocity impact. Belingardi and Vadori [10] have examined that for glass-fiber-epoxy matrix laminated plates subjected to low velocity impact loads, the first damage force and maximum force are

* Corresponding author.
E-mail address: ankushsharma260785@gmail.com (A.P. Sharma).

https://doi.org/10.1016/j.heliyon.2019.e02706
Received 16 May 2019; Received in revised form 18 September 2019; Accepted 17 October 2019

substantially equal for two types of unidirectional reinforced layers and three types of fabric reinforced layers, respectively. Rio et al. [11] have examined that for laminates made of carbon fiber reinforced epoxy (CFRP), their cooling before impact exhibits a larger amount of damage and this is comparable to that of increasing the energy of impact and does not go with larger energy dissipation. Hosseinzadeh et al. [12] have examined that for plates subjected to impact energy level of 30 J, CFRP shows no damage, whereas glass fiber reinforced epoxy (GFRP) exhibits failure. They have also observed that for carbon/glass/epoxy plates, low and high velocity impacts do not exhibit damage and collapse, respectively. Mitrevski et al. [13] have investigated that for thin woven CFRP laminates, the largest damage area is produced by the blunt hemispherical impactor, followed by ogival and conical impactors for all low velocity impact conditions.

Babu et al. [14] have reported that woven GFRP laminates show the highest and lowest ballistic limits under truncated-nose and sharp-nose projectiles impact, respectively. Aktaş et al. [15] have reported that in case of unidirectional GFRP laminates of different stacking sequences, $[0/90/0/90]_s$ is found to be having higher penetration threshold than that of $[0/90/45/-45]_s$. They have reported that higher impact energies exhibit fiber fracture as the primary damage mode, whereas smaller impact energies exhibit delamination and matrix cracks resulting from indentation. Sevkat et al. [1] have investigated that glass-skin/graphite-core type performs a little better on impact than graphite-skin/glass-core type and both these hybrid specimens perform better than graphite but not as well as for glass. Icten et al. [16] have reported that quasi-isotropic GFRP plates are having nearly same impact response and damage tolerance at all temperatures (20 °C, -20 °C and -60 °C) up to impact energy level of 20 J. Sayer et al. [17] have reported that carbon glass (CG) hybrid composite impacted from surface with carbon fibers is seemed to having smaller energy absorption capability and approximately 30 % higher perforation threshold to that of glass carbon (GC) hybrid composite impacted from surface with glass fibers. Karakuzu et al. [18] have reported that the energy absorption capability of GFRP plates under the impact of equal mass is lower than that of equal velocity. Akin and Senel [19] have investigated that for cross-ply and angle-ply GFRP plates, clamping the material at its four sides makes a more stable structure with more distribution of damage at bottom of the samples compared to two side clamping.

Evci and Gülgeç [20] have reported that for woven and unidirectional E-Glass composites, woven laminates are having higher ultimate strength, on-set of perforation and perforation energy limits, low velocity impact limit along with greater initial failure (Hertzian failure) force, main damage (maximum) force, and smaller damaged area. They have investigated that the best impact performance is exhibited by Aramid composites. Soliman et al. [21] have reported that incorporating functionalized multi-walled carbon nanotubes (MWCNTs) with carboxyl group (COOH) to woven CFRP composites, below penetration limit, penetration energy is improved by 50 % with same peak force using 1.5 % COOH-MWCNTs by weight of epoxy which results into increasing energy absorption by 50 %. They have also observed that the impact response and damage size of composites are enhanced and limited, respectively by adding functionalized MWCNTs. Quaresimin et al. [22] have reported that for woven CFRP laminates, lay-up and impact energy do not influence matrix-controlled event and parameters such as initiation of damage as well as DTL and concomitant energy, however, the thickness of the laminate does influence them. They have also examined that the absorbed energy increases with the thickness of the laminates and improves by being of 0/45 interfaces. Meo et al. [23] have reported that the resistance to damage, ductility, toughness and absorbed energy levels before the failure of structures made of composites are observed to increase by embedding shape memory alloy (SMA) wires into composites compared to conventional structures made of composites. Rahman et al. [24] have reported that incorporating amino-functionalized MWCNTs (NH_2-MWCNTs) to GFRP composites, increase in ballistic limit velocity by about 6 % and energy absorption capability are observed by adding 0.3 wt. % (weight percentage) loading of MWCNTs whereas this velocity does not increase by higher wt. % loading of MWCNTs. They have observed that damage tolerance is increased considerably exhibiting the lower size of damage by adding MWCNTs.

Zhang et al. [25] have reported that for composite laminates formed of Ultrahigh Molecular Weight Polyethylene (UHMWPE) filaments, better energy absorbed capacity and damage resistance to impact are exhibited by single-ply 3D orthogonal woven fabric than that of unidirectional and 2D plain-woven fabric. Taraghi et al. [26] have reported that in case of woven Kevlar/epoxy laminated composites, energy absorption at ambient (27 °C) and low (-40 °C) temperatures is increased up to about 35 % and 34 % by adding MWCNTs of 0.5 wt. % and 0.3 wt. %, respectively, whereas, bending stiffness is correspondingly increased up to about 15 % and 13 %. Agarwal et al. [27] have discussed a comprehensive review for FRP composite material in a broader area of damage induced by impact. Namala et al. [28] have examined that for GFRP composite, cross-ply and unidirectional laminates exhibiting corresponding lower and higher deformations are having rounded rhombus and elliptical like damage profile shapes on the back face which are symmetrical about the impact point. Sarasini et al. [29] have reported that better energy absorption capability and improved tolerance to damage are exhibited by hybrid laminates having an intercalated configuration of basalt and carbon fabrics with their alternative sequence compared to laminates with all-carbon fabric layers. Sikarwar et al. [30] have reported that for GFRP laminates of different thicknesses and lay-up sequences, (0/90) is having the highest impact resistance. In their study, laminates exhibit increased ballistic limit and energy absorption capability by increasing dynamic Young's modulus and failure strain.

Balaganesan et al. [31] have reported that GFRP laminates exhibit higher energy absorption capacity with nano clay up to 5 wt. % of the matrix under the projectile impact. Azzam and Li [2] have investigated that in case of unidirectional CFRP laminates of different stacking sequences on low velocity impact, C-scan images of upper faces of $[0/90/-45/45]_{2s}$ and $[0/90/-45/45]_s$ exhibit lower area of failure, delamination, indentation in the damage location and sensitivity of damage size than that of $[45/45/90/0]_{2s}$ and $[45/45/90/0]_s$. Reghunath et al. [32] have investigated that better impact resistance of woven GFRP composites is achieved by fiber volume fraction of 43–44 %. Singh and Singh [33] have presented a detailed review of impact behavior and analysis of FRP composite. Evci [34] has reported that for glass fiber reinforced polyester resin laminates, woven composites are having superior damage resistance and higher load bearing capacity in terms of Hertzian failure force (delamination) and main failure force (laminate failure), respectively than that of unidirectional composites. He has examined that the laminates with their initiation, progress of damage and effective damage modes in terms of these forces closely depend on the energy of impact and thickness of the laminate. Singh et al. [35] have reported that quasi-isotropic symmetric and asymmetric GFRP laminates are having corresponding absorb energy of 59.7 J and 45.98 J which are higher than that of laminates suggested by various researchers.

Bandaru et al. [36] have reported that for similar areal density of three-dimensional (3D) and two-dimensional (2D) Kevlar/polypropylene laminates, a higher peak load (14.21–30.25 %), more absorption of energy (12.7–26.2 %) and lower formation of cone at back of the target (25–39 %) are exhibited by 3D angle interlock composite than that of 3D orthogonal and 2D plain woven composites. Singh et al. [37] have reported that in case of asymmetric laminate with quasi-isotropic lay-up for plain CFRP, absorbed energy and damage area are correspondingly increased by 13.53 % and reduced on doping of 2 wt. % of MWCNTs, while doping of 5 wt. % of MWCNTs cause this energy to decrease by 10.49 %. Bandaru et al. [38] have reported that higher, lower and intermediate peak forces are exhibited by basalt 3D (B3D), Kevlar 3D (K3D) and hybrid 3D (Kevlar/basalt/PP) (H3D) composites, respectively, however, more energy absorption is exhibited by H3D composites. Hazzard et al. [39] have investigated that for thin Dyneema composite laminates subjected to low velocity impact, the largest back face

deflection is exhibited by [0°/90°] cross-ply laminate, whilst central deflection is reduced by an average of 43 % for quasi-isotropic architectures exhibiting great reduction in time taken to maximum back face deflection and having smaller impact damage zones of up to 37.5 % as compared to that of [0°/90°]. Sikarwar et al. [40] have investigated that an improvement of 20 % in specific energy absorption is observed for glass/kevlar/epoxy laminates in which percentage of kevlar is 27.5 % w/w when compared to the laminates of GFRP for equal initial velocities of 170 m/s.

In literature review it is observed that impact resistance of laminates has been tried to improve by various researchers in different means such as changing of fabric to be reinforced, making of composites based on core or use of reinforcements that are to be additional (nano-fillers) like single-walled carbon nanotubes (SWCNTs) or MWCNTs. In this study, the resistance to impact has been attempted to improve by altering the sequence of stacking of laminates. In this context, the effect of separation of fiber orientation through the thickness on low velocity impact behavior of composites is characterized in terms of force-displacement response, damage and performance parameters. Two different layups of composites of the same thickness are fabricated using unidirectional (UD) GFRP. Drop tower impact machine is used to perform low velocity impact tests at six different levels of energy. The following sections present the details of the work.

2. Experimental

2.1. Materials

UD E-glass fiber mat supplied by Courtaulds Advanced Materials (Holdings) Ltd., UK, is used as the reinforcement material. The areal density and volume density (calculated using the Archimedes method by weight [41]) of UD glass fiber used are 551 g/m^2 and 2.17 g/cc respectively. Epoxy LY 556 and hardener HY 951 (supplied by Huntsman India Private Ltd.) in the ratio of 100:10 parts by weight, respectively are used as the matrix. Tables 1 and 2 show the properties of epoxy and plain composite.

2.2. Manufacturing procedure

In case of [0/90/90/0] composite denoted by C1 in which two layers with fibers having 0° orientations are separated by two layers with fibers having 90° orientations. In this case, four UD fiber layers each of size 350 × 350 mm^2 are cut out from a UD roll. First, a Mylar sheet is placed over a flat plate. After applying a layer of epoxy on this, a fiber layer is placed and epoxy is applied to it using a brush. Then another fiber layer with its orientation perpendicular to the first one is placed and epoxy is applied. This process is repeated for the remaining two fiber layers. Then over this, Mylar sheet is placed and the whole assembly is pressed using a roller to spread the epoxy uniformly and to squeeze out any excess epoxy. Four spacers each with 2 mm thickness are placed at four corners of the layup which is located inside the vacuum bag between two platens of a hydraulic press. This is followed by curing for 24 hours at room temperature with an applied pressure of up to 48 kgf/cm^2 and the vacuum pump reaches up to 650 mm of Hg. Similarly, [90/-45/45/0] composite is also made in which two layers with fibers having 90° and 0° orientations are separated by two layers with fibers having -45° and 45° orientations and is denoted by C2. The fiber volume fraction obtained from the burn test is 50 %. The final thickness of the composite laminate obtained is 2 mm. The specimens of size 100 × 100 mm^2 are cut using water-cooled slicing saw for low velocity impact tests from the prepared 350 × 350 mm^2 sheet. For further information, Ref. [42] can be followed.

Table 1
Properties of epoxy.

Material	Elastic modulus (GPa)	Poisson's ratio	Density (kg/m^3)	Viscosity (cP) at 25 °C	Pot life (min)
Epoxy	3.40	0.36	1200	1700	45

Table 2
Elastic properties of the unidirectional laminate.

Material	E_{11} (GPa)	E_{22} (GPa)	ν_{12}	ν_{21}	G_{12} (GPa)
UD GFRP	30.5	6.34	0.29	0.06	2.38

2.3. Testing

The test is performed using an INSTRON CEAST 9340 drop tower impact testing machine (photograph is shown in Fig. 1a). The details of the clamping mechanism and fixture can be found in Ref. [42]. The impact device includes a rigid base, a drop-weight impactor, a rebound catcher and a guide mechanism.

The acquisition rate and the duration of data collection used are 200 kHz and 25 milliseconds, respectively. The specimens are tested as per ASTM standard D5628 (FA) [43] and are clamped on a fixture along a circumference of 70 mm diameter. A schematic drawing of the experimental set-up of the low velocity impact tests is shown in Fig. 1b. A hemispherical steel impactor with a tip of 16 mm diameter and a total mass of 3.132 kg is used. The composite plates are subjected to low velocity impact loading at energy levels of 5 J, 10 J, 15 J, 20 J, 25 J, and 30 J. The corresponding impact velocities are 1.79 m/s, 2.53 m/s, 3.10 m/s, 3.57 m/s, 3.99 m/s and 4.38 m/s respectively. During the test, the recording of the time history of impact force and velocity of the impactor before impacting the specimen is performed. The various parameters of interest are generated using this information and the mass of the impactor [10, 43]. After the test, visual inspection is performed for the carefully preserved samples by taking images of the front (impacted) and rear (non-impacted) surfaces of damaged composites.

3. Results

3.1. Force-displacement response and damage

In this section, the results of [0/90/90/0] and [90/-45/45/0] laminates are described under impact loading.

In case of impact energy of 5 J, force-displacement responses shown in Fig. 2a represents large oscillations for C1 and C2 before recording corresponding maximum forces of about 2343 N and 2365 N. These represent first material damage within composites in the form of delamination, front surface cracks or front surface indentation [10]. The initiation of delamination failure probably causes the first damage threshold [44]. The force initially increases till it reaches the peak load and decreases during unloading with monotonic reductions in force and displacement. The force-displacement graphs show closed loops for C1 and C2 exhibiting corresponding higher and lower residual displacements of about 3 mm and 2.4 mm. Small deformation of top and bottom composite layers leads to the formation of dent near the impact location which is slightly higher for C1 than C2. In case of force-displacement responses, almost all the energy is released back from the specimen to the impactor showing good impact resistance characteristics for C2 to that for C1. The rate of impact energy represents the rate of loading for composites. It provides the stiffness of the laminates in terms of their energy history obtained at each impact energy level indicating the type of loading rate during impact, i.e., static or dynamic. Therefore, energy history data is used in its linear part before reaching the peak load to calculate this rate. The rate of impact energy comes out to be 1.80 J/ms and 1.91 J/ms for C1 and C2, respectively implying a static loading rate.

Figs. 3, 4, and 5 illustrate images of damaged surfaces of composites on front and rear faces. In case of C1, the overall damage area of impact face with matrix cracks, delamination, and fibers breakage are shown by dark black lines (Fig. 3). In case of C2, the damage area on the front and

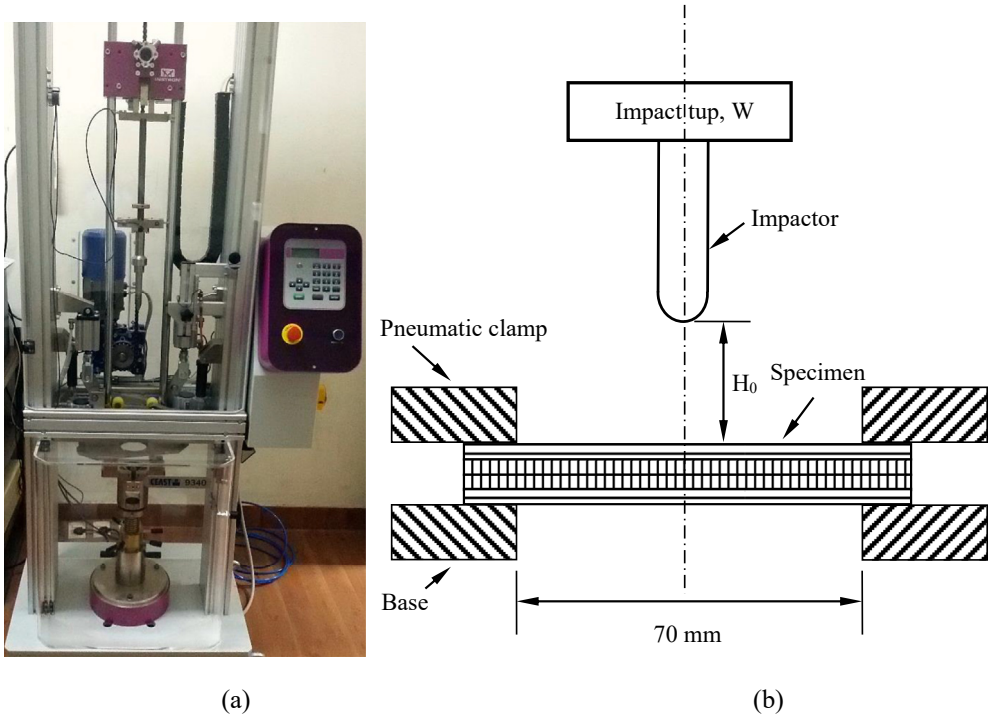

Fig. 1. (a) Photograph of Instron CEAST 9340 drop tower, (b) schematic diagram of the experimental set-up for impact tests.

rear faces are shown by continuous and discontinuous black lines, respectively (Fig. 5). Here, top (impacted) and bottom (non-impacted) layers of fibers are represented by t and b. From these pictures, the following observations can be depicted through visual examinations. In case of C1, matrix cracking is occurred through 90° plies, whereas, for C2, it has occurred through 90°, 45°, and -45° plies. At this energy level for C1, the symmetric cross-ply material shows damage in the form of two leaf clover on rear face exhibiting equal amount of a peanut shape delamination area between [0/90] and [90/0] layers with its major axis orienting along 0°/90° fiber directions, respectively (Fig. 4a) [45, 46]. Whereas C2 is having two leaf clover on the rear face exhibiting an equal amount of peanut shape delamination area between [-45/90] and [45/0] layers with its major axis orienting along -45°/45° fiber directions, respectively (Fig. 5a) [46]. This is discussed in Section 4 using classical laminate theory. More damage is developed towards the rear face of laminates than that of the front face. The resulting delamination area is observed to be lower for C2 than that for C1 (Figs. 3a, 4a, 5a). It is to be noted that a change in ply orientations causes delamination due to bending stiffness mismatch of adjacent layers [47, 48].

In case of impact energy of 10 J, the overall shape of force-displacement curves shown in Fig. 2b is similar for C1 and C2 to that at 5 J impact energy level (Fig. 2a) until attaining corresponding lower and higher maximum forces of about 3557 N and 4008 N. Force with small plateau can be seen around maximum value for C1, however, this cannot be seen for C2. These are followed by monotonic reductions in force and displacement for C1 and C2 during unloading exhibiting corresponding higher and lower residual displacements of about 3.9 mm and 2.9 mm. C1 and C2 are having the rate of impact energy of 4.3 J/ms and 4.6 J/ms representing a static loading rate. More amount of damage is visible on the front and rear faces to that at 5 J and their typical shapes are shown in Figs. 3b, 4b, 5b. Specifically, C1 is having the formation of rear surface cracks with its major axis orienting along 0° fiber direction, whereas, they are not observed for C2.

In case of impact energy of 15 J, force-displacement responses shown in Fig. 2c are having softening observed for C1 before reaching the maximum force of about 3976 N. Whereas softening is not observed for C2 exhibiting the higher maximum force of about 4909 N to that for C1. In case of C1, the extent of matrix cracking, fibers failure in contact region and length of rear surface cracks majorly orienting along 0° fiber direction is higher than that of C2 whose major axis is oriented along -45°/45° fiber directions (Figs. 3c, 4c, 5c). This results in the dropping of forces after attaining peak loads for composites (Fig. 2c). During unloading, C1 and C2 follow monotonic reductions in force and displacement from about 2544 N and 2650 N. The internal damage evolution can be attributed to this behavior [49]. C1 and C2 are having higher and lower residual displacements of about 5.3 mm and 4.9 mm. The rate of impact energy for C1 and C2 is 6.8 J/ms and 7.6 J/ms indicating a static loading rate.

In case of impact energy of 20 J, force-displacement responses shown in Fig. 2d exhibit corresponding maximum force levels of about 4578 N and 5641 N following steep drops to 2407 N and 3466 N for C1 and C2. Subsequently, displacement is increased and force oscillates about a constant value just before unloading. These correspond to plies of C1 and C2 with their patches being pushed out on the bottom layer majorly orienting along 0° and -45°/45° fiber directions, respectively. This separation (fibers splitting) occurring due to higher energy of impactor (20 J) seems to be more for C1 to that for C2 [1]. This results in an appreciable reduction in the impact resistance of C1 (out-of-plane stiffness) to that of C2 exhibiting sudden drops in force-displacement histories. Decohesion of fiber matrix is observed in about all the layers for C1 noticing a little trace of an initial perforation (approaching saturation), whereas, it is about to happen for C2 (Figs. 3d, 4d, 5d). Maximum displacements are correspondingly noted to be higher and lower of about 8.9 mm and 8.3 mm for C1 and C2. The impactor is rebounded because of the remaining resistance of C2 which is strong enough to that of C1. This yields more force and less residual displacement of about 4.8 mm for C2, whereas, this displacement is about 6.8 mm for C1. C1 and C2 are having a respective rate of impact energy of 9.3 J/ms and 10.2 J/ms signifying static rate of loading.

In case of impact energy of 25 J, force-displacement responses presented in Fig. 2e exhibit corresponding maximum forces of about 5134 N and 5785 N for C1 and C2 following sharp drops to 3241 N and 3114 N. This is followed by a somewhat more gradual decrease in force with increasing displacement for C2 to that for C1. Subsequently, this is

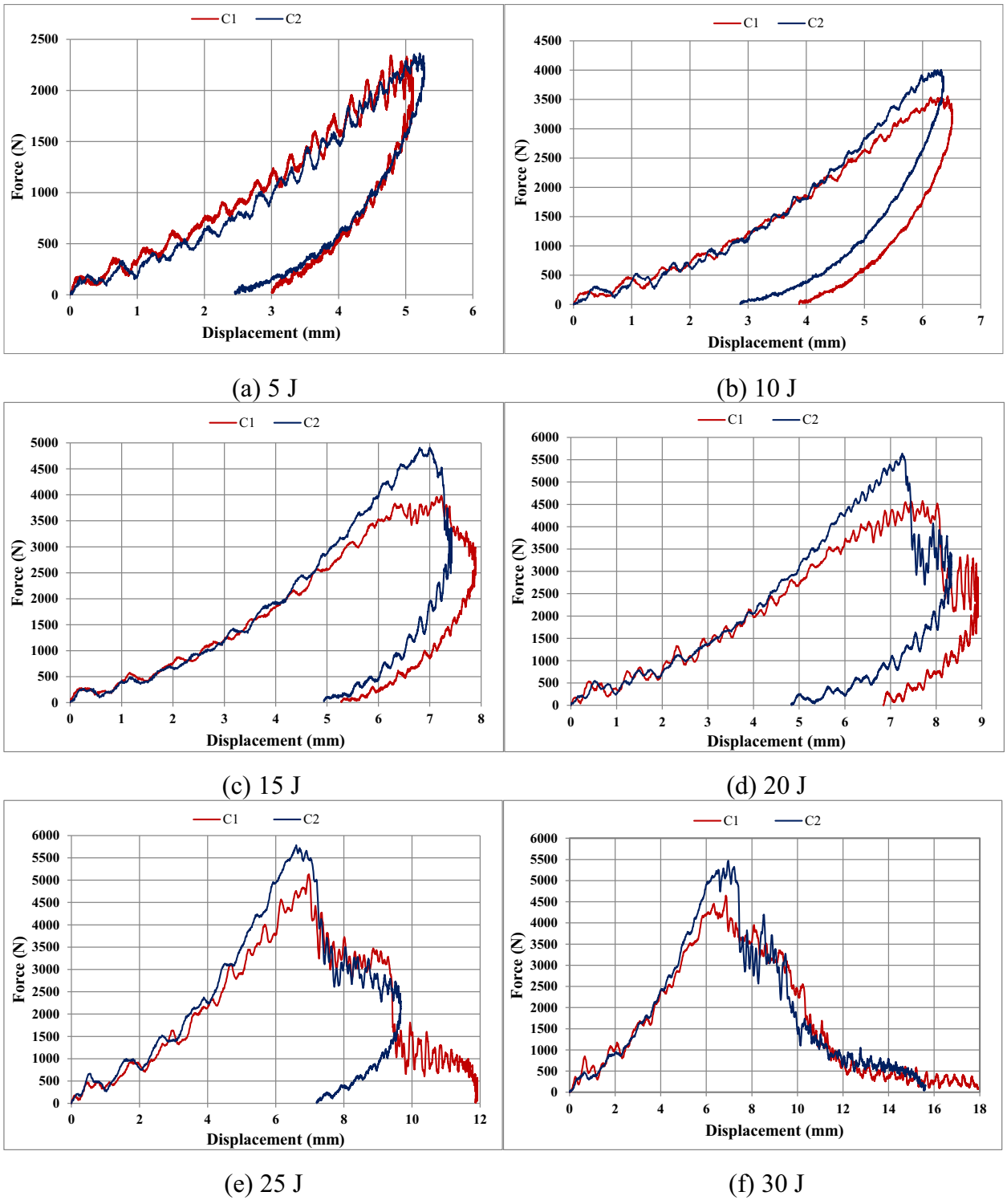

Fig. 2. (a–f) Force-displacement response for composites impacted at various energy levels.

continued for C1 exhibiting another sharp drop to 1027 N following oscillation of force about a constant value with increasing displacement. Whereas C2 is having monotonic reductions in force and displacement after attaining the force of about 2500 N. The laminate is about to penetrate for C1 and is not seemed to happen for C2. In case of C1, fibers with a vertical patch of ply being separated on the bottom layer are majorly oriented along 0° fiber direction as can be seen in Fig. 4e. Whereas, in case of C2, this separation (fibers splitting) is lower than that of C1 and is majorly oriented along -45°/45° fiber directions (Fig. 5e). These are well correlated with the behavior of composites exhibiting sharp drops in forces as stated before (Fig. 2e). C1 and C2 are having higher and lower residual displacements of about 11.9 mm and 7.2 mm. The corresponding rate of impact energy for C1 and C2 is 11.6 J/ms and 14.1 J/ms implying a static rate of loading. In case of C1, in addition to front fibers cracks, fibers failure are occurred exhibiting some amount of perforation (Figs. 3e, 4e), whereas, this partial perforation is about to happen for C2 (Fig. 5e).

In case of impact energy of 30 J, force-displacement responses shown

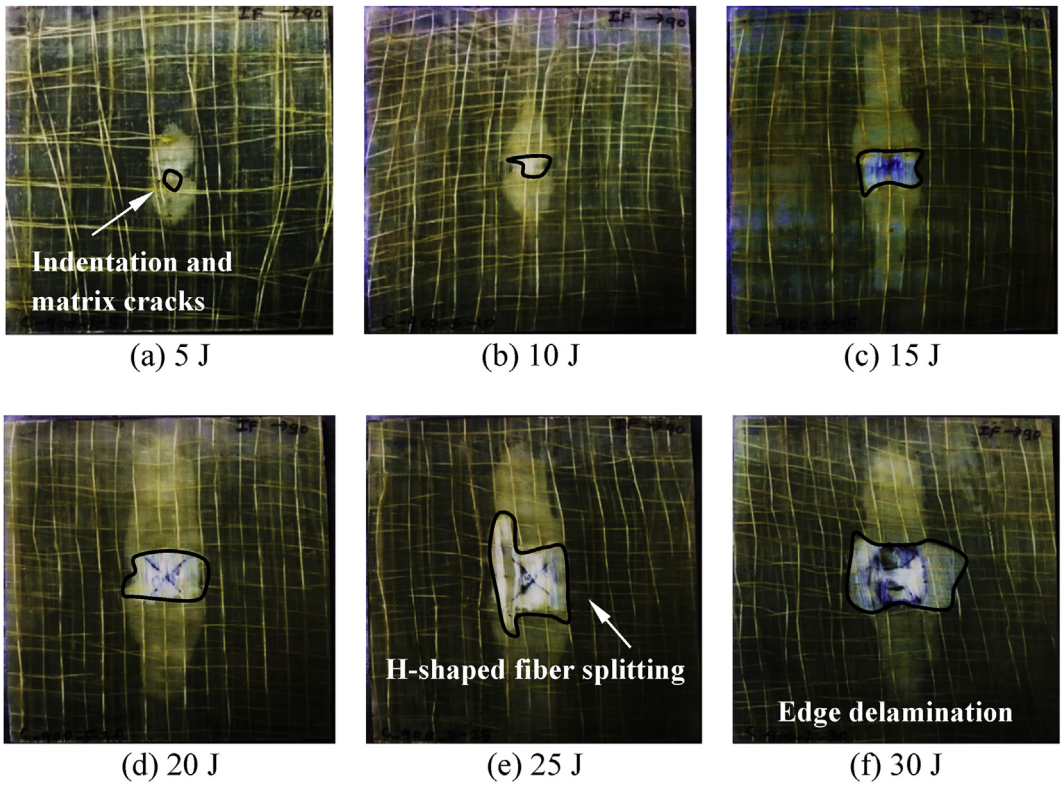

Fig. 3. (a–f) Damage patterns of C1 on the front face (↑ 0° direction).

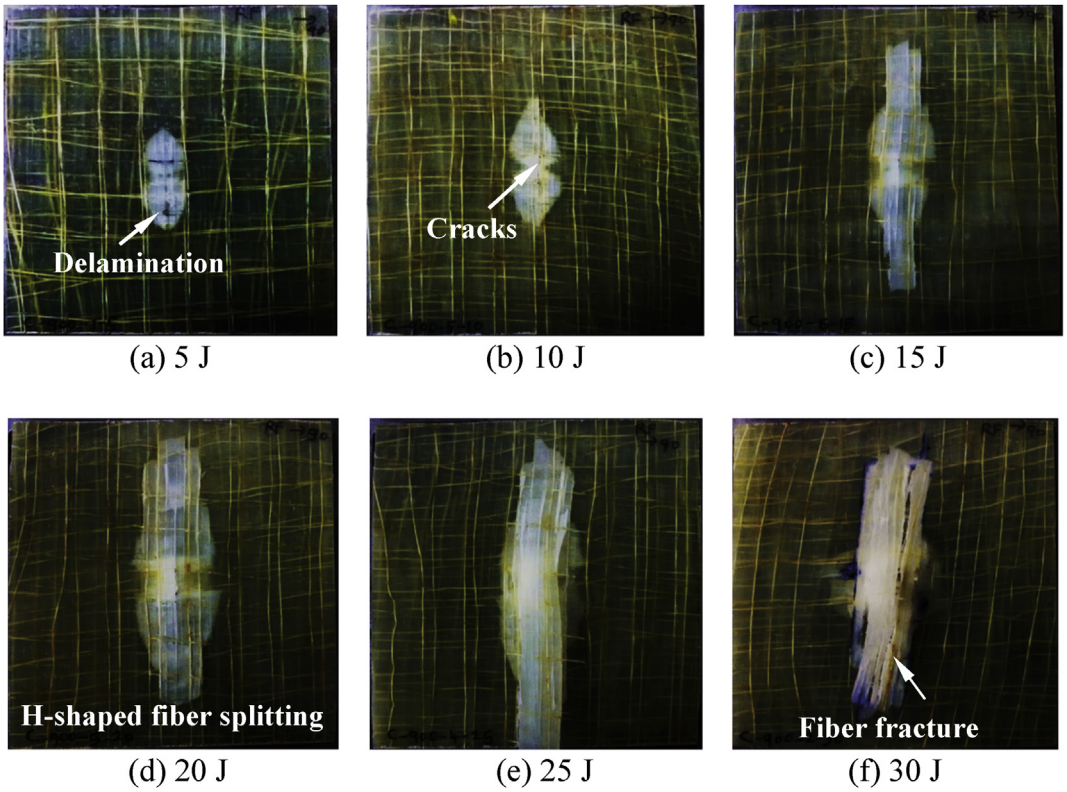

Fig. 4. (a–f) Damage patterns of C1 on the rear face (↑ 0° direction).

in Fig. 2f represents more gradual reductions in forces for C1 and C2 to that at 25 J with increasing displacement after attaining corresponding maximum forces of about 4648 N and 5472 N. In case of C1, vertical patch of fibers is separated on bottom layer to a large extent against 25 J of impact energy resulting into fibers fracture majorly orienting along 0° fiber direction as can be seen in Fig. 4f. Whereas, in case of C2, this

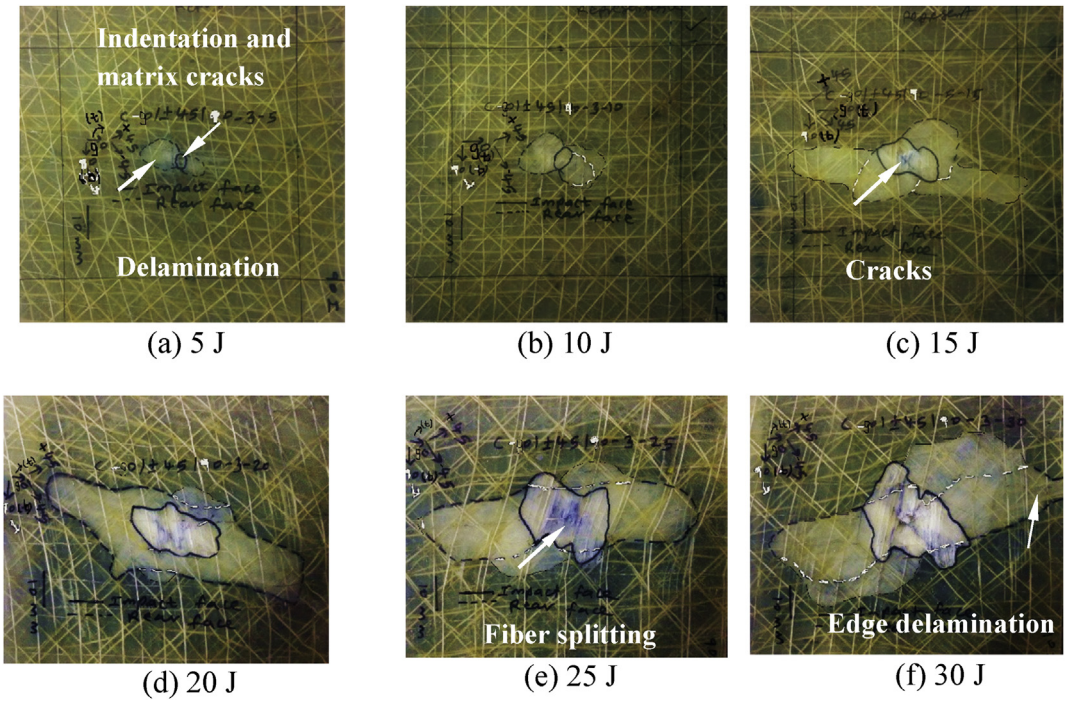

Fig. 5. (a–f) Damage patterns of C2 on front and rear faces (↘ -45° direction).

separation (fibers splitting) is lower than that of C1 with its major axis orienting along -45°/45° fiber directions (Fig. 5f). This is well connected with the behavior of force-displacement curves for composites after attaining maximum forces (Fig. 2f). Composites exhibit constant regions (almost open type curves) after gradual dropping of forces in force-displacement curves revealing completely softening parts. This is happened due to energy dissipation which occurs due to friction until impactor stops. This plateau is particularly observed for C1 and C2 after attaining corresponding displacements of about 12.2 mm and 12.7 mm which do not seem to be real ones. The final impactor displacement for C1 and C2 is correspondingly reached to about 18 mm and 15.6 mm. This is identical to the case of perforation for C1 which is defined as small energy increment beyond the saturation of load carrying capacity of the plate. However, in case of C2, perforation is about to take place representing its more impact resistance to that of C1. C1 and C2 are having the rate of impact energy of 13.3 J/ms and 16.2 J/ms demonstrating static rate of loading. Overall, mechanism of major energy absorption is delamination and matrix cracks which are observed as prominent damage modes at lower impact energy levels (up to 15 J). However, these modes are appeared to be splitting and fracture among fibers at higher impact energy levels (more than 15 J to up to 30 J) representing in a schematic diagram in Fig. 6 [15]. Corresponding rear (non-impacted) side and cross-sectional views of damaged specimens are depicted in this Figure.

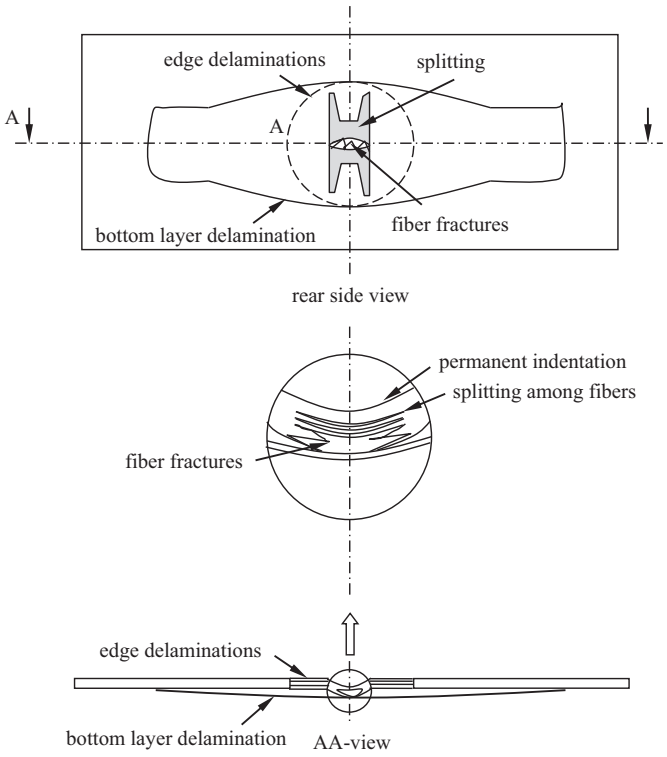

Fig. 6. Schematic diagram of different damage modes for composites [15].

3.2. Performance parameters

In this section, the performance of composites are presented in terms of parameters such as first damage and maximum forces, maximum displacement, permanent deformation, first cracking energy, bending stiffness, elastic and residual displacements, elastic strain energy, damage degree, square-root delaminated area, delamination length, delamination width and contact duration [10].

Fig. 7a shows damage degree of composites versus impact energy which is the ratio of energy absorbed by the specimen to the impact energy. The area enclosed inside a force-displacement response is calculated to obtain energy absorbed. Matrix cracks, fiber fracture, fiber-matrix debonding and layer delamination are the various damage mechanisms through which composites absorb energy. It can be observed that C1 is having higher damage degree to that of C2 up to 25 J impact energy (Fig. 7a). It means that absorbed energy increases by separating fiber orientation at levels of energy lower than the perforation limit. The data points are overlapped for composites at the highest impact energy level of 30 J indicating that energy of very little amount is present for ricochet of the impactor implying perforation limit has reached. The

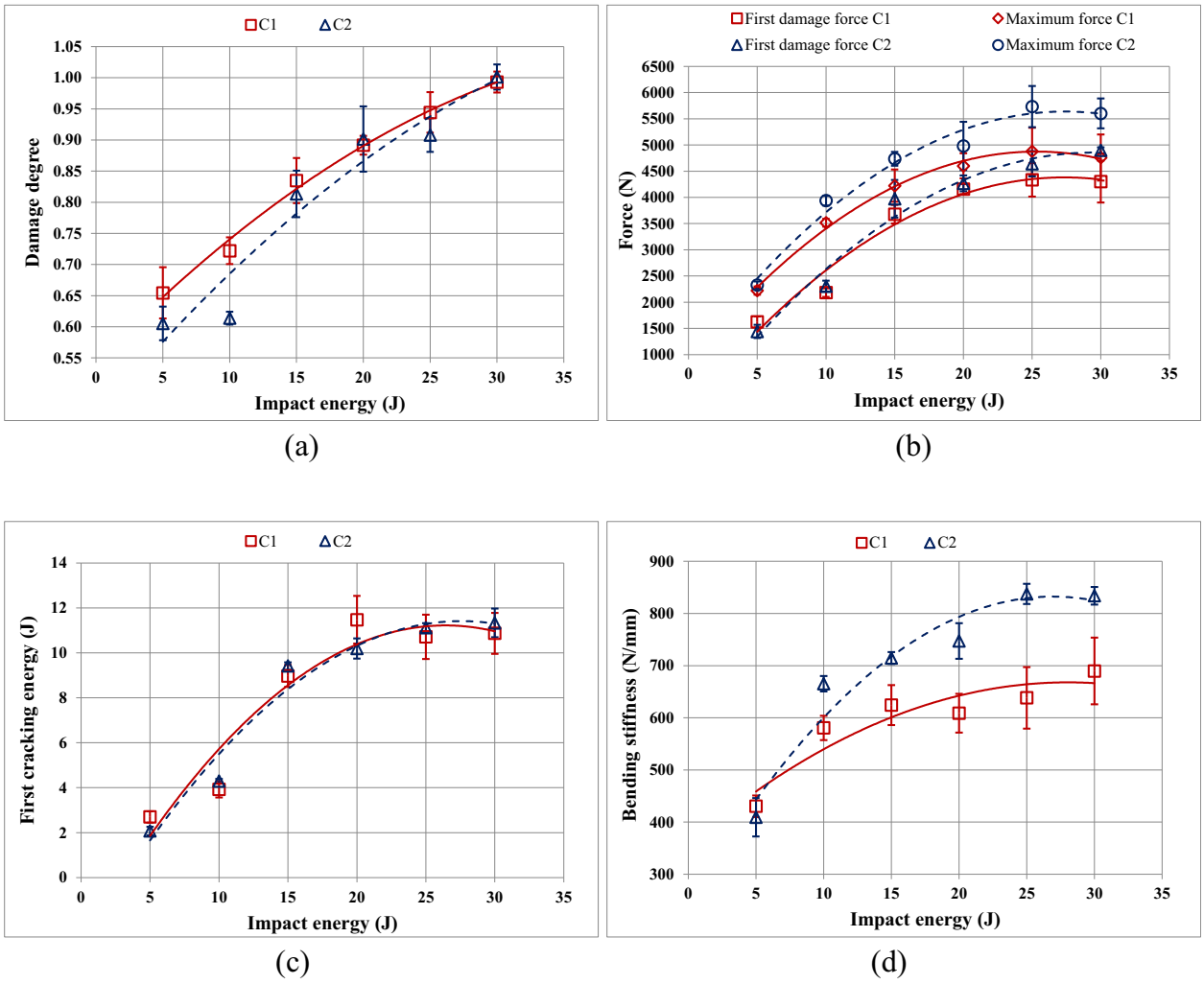

Fig. 7. Variations of (a) damage degree, (b) first damage force and maximum force, (c) first cracking energy and (d) bending stiffness for composites against impact energy.

experimental points are well-fitted by second-order polynomials. This trend of composites matches to that reported in Ref. [10]. Therefore, the separation of fiber orientation does affect the level of damage degree.

The first damage force is DTL which is defined as load level at which more oscillations occur before reaching the maximum force and is recognized from the force-displacement response at a given impact energy level (Fig. 2). DTL of composites is plotted in Fig. 7b against impact energy. In this case, for a given level of impact energy, C2 is having more DTL to that of C1. In case of composites, DTL first increases with increasing levels of impact energy and then starts saturating which is being more drastic in case of C1. The experimental data points represent a general quadratic trend. Similarly, a variation of the maximum force of composites against impact energy presented in Fig. 7b follows the comparable trend to that of variation of first damage force against impact energy. However, for a given level of impact energy, the maximum force of composites is higher than that of the first damage force. C2 is having a higher maximum force to that of C1 at all energy levels. Therefore, separation of fiber orientation through the thickness has a noticeable effect on levels of DTL and maximum force. The first cracking energy (fce) of composites presented in Fig. 7c is energy corresponding to the first damage force at a given impact energy level [50]. As a result, in this case, composites follow a similar trend to that of variation of first damage force as a function of impact energy, i.e., fce is higher for C2 and lower for C1 at all energy levels. Therefore, the separation of fiber orientation does have an effect on the level of first cracking energy. As far as delamination resistance [48] and perforation resistance [51] are considered, bending stiffness has been found as an important parameter. The impact bending stiffness of laminated composites presented in Fig. 7d is obtained from the slope of the ascending section of force-displacement response in its linear part before reaching a peak load at a given impact energy level (Fig. 2(a–f)) [52]. In this case, for a given level of impact energy, bending stiffness is higher for C2 and lower for C1. The bending stiffness increases with increasing levels of impact energy and then starts saturating which is being more radical in case of C1. Therefore, the separation of fiber orientation through the thickness does have a marked effect on the level of bending stiffness.

Fig. 8a presents typical force-displacement and energy-displacement responses of C1 at an impact energy level of 5 J. In this case, elastic strain energy and energy dissipated by damage have been obtained from this energy-displacement response following a rebound of impactor [53]. The variation of elastic strain energy of composites against impact energy is presented in Fig. 8b and first increases with increasing levels of impact energy and subsequently start decreasing. At a given impact energy level, it is apparent that the elastic strain energy of C2 is higher than that of C1 at energy levels lower than the perforation limit of 30 J. The damage degree presented in Fig. 7a represents energy absorbed by composites as stated before which is also energy dissipated by damage shown in Fig. 8a. In this case, C1 is having higher energy absorbed to that of C2 at energy levels lower than perforation limit of 30 J. Similarly, elastic and residual displacements have been extracted from the force-displacement response

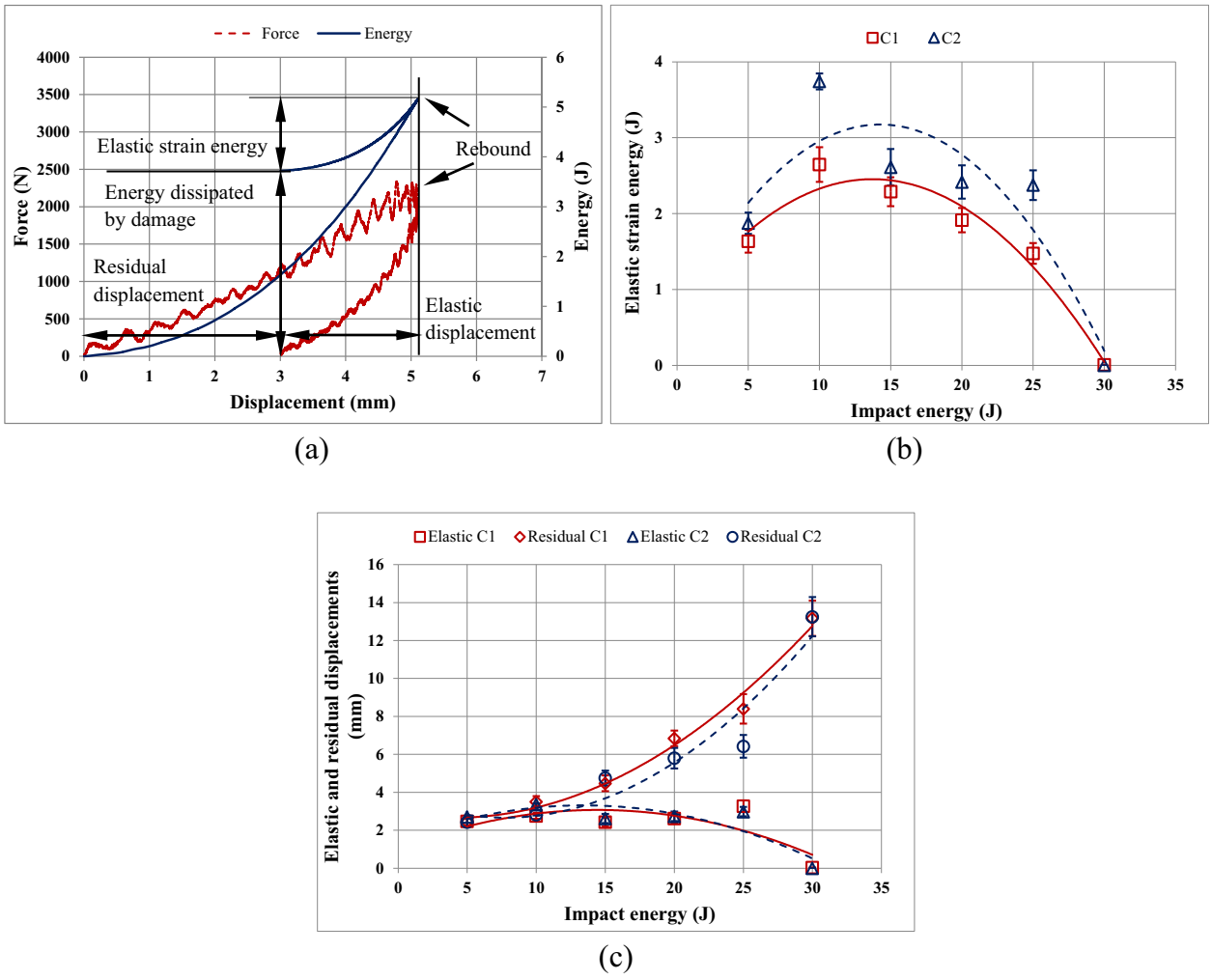

Fig. 8. (a) Force and energy versus displacement for C1 composite, (b) elastic strain energy and (c) elastic and residual displacements for composites at various impact energy levels.

shown in Fig. 8a following a rebound of the impactor. The variation of these displacements for composites against impact energy is shown in Fig. 8c. This follows a comparable trend to that of variations of elastic strain energy and energy absorbed by laminates against impact energy as shown in Figs. 7a, 8b. It means that C2 and C1 are having corresponding higher elastic and residual displacements at energy levels lower than the perforation limit of 30 J.

The maximum displacement of composites obtained from force-displacement curves is shown in Fig. 9a as a function of impact energy and increases with increasing levels of impact energy seeming higher for

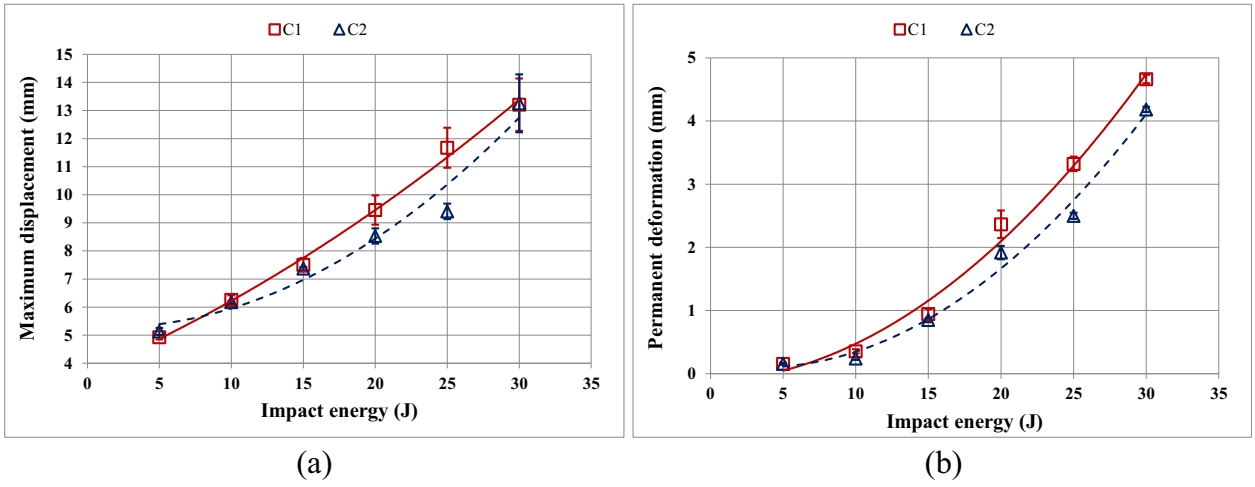

Fig. 9. (a) Maximum displacement and (b) permanent deformation for composites at different impact energy levels.

C1 and lower for C2. The difference in maximum displacement between composites increases with increasing levels of impact energy before attaining perforation limit of 30 J. The permanent deformation measured on the rear face of composites following removal of samples from supports is shown in Fig. 9b as a function of impact energy. Again, at a given level of impact energy, a lower level of permanent deformation is exhibited by C2 to that of C1. Interestingly, the considerable difference is observed at higher levels of impact energy. The extensive fiber fracture on the rear face is responsible for higher levels of permanent deformation for C1 at higher levels of impact energy. Therefore, separation of fiber orientation does have a clear effect on levels of maximum displacement and permanent deformation.

ImageJ software is used to measure the delamination area of each plate of composites. The real scale image of composites is exported to this software after marking the designated area on them as shown in Figs. 3, 4, and 5. To reduce the error to a minimum, the respective contour is drawn with great magnification. The irregular area is manually traced on the same image close to three times using a polygon option inbuilt in the above software. The average of these areas is shown in Fig. 10a providing their desired estimates. The general trend of almost a straight line is noticed for the relationship between the square-root delaminated area and the impact energy. This delaminated area of composites increases with increasing impact energy levels both on impact and rear faces and seems to be more on rear face to that on impact face. Particularly, this area on both impact and rear faces is lower for C2 and higher for C1 at all energy levels as can be seen in Fig. 10a. The major delamination length (L) of composites is shown in Fig. 10b as a function of impact energy and is traced on impact and rear faces correspondingly along 0° and -45° fiber directions for C1 and C2. L increases for composites with increasing levels of impact energy. In case of impact face, for a given level of impact energy, C2 is having higher L to that of C1. Whereas, in case of the rear face, C1 is having higher L to that of C2. The difference in L between composites increases with increasing levels of impact energy. L shows a general trend of nearly a straight line on impact and rear faces. The major delamination width (W) of composites is shown in Fig. 10c as a function of impact energy and is traced on impact and rear faces along 90° and 45° fiber directions for C1 and C2, respectively. W of composites increases with increasing levels of impact energy. In case of impact face, for a given level of impact energy, C1 is having higher W to that of C2. However, in case of the rear face, C2 is having higher W to that of C1. The difference in W between composites increases with increasing levels of impact energy. Therefore, separation of fiber orientation does have an effect on levels of square-root delaminated area, delamination length and delamination width, particularly on the rear face. The contact duration of composites is shown in Fig. 10d as a function of impact energy and decreases initially and then increases with increasing levels of impact energy. The contact duration is higher for C1 and lower for C2. The difference in contact duration between composites increases with increasing levels of impact energy before reaching perforation limit of 30 J due to increased engaging time of impactor and composites. The contact duration follows a general trend of quadratic nature against impact energy. Therefore, the separation of fiber orientation does influence the level of contact duration. The error bars in the form of standard deviations for performance parameters of composites discussed above are shown in Figs. 7, 8, 9, and 10 at different impact energy levels. These values are from a minimum of three tests for each layup of the composite.

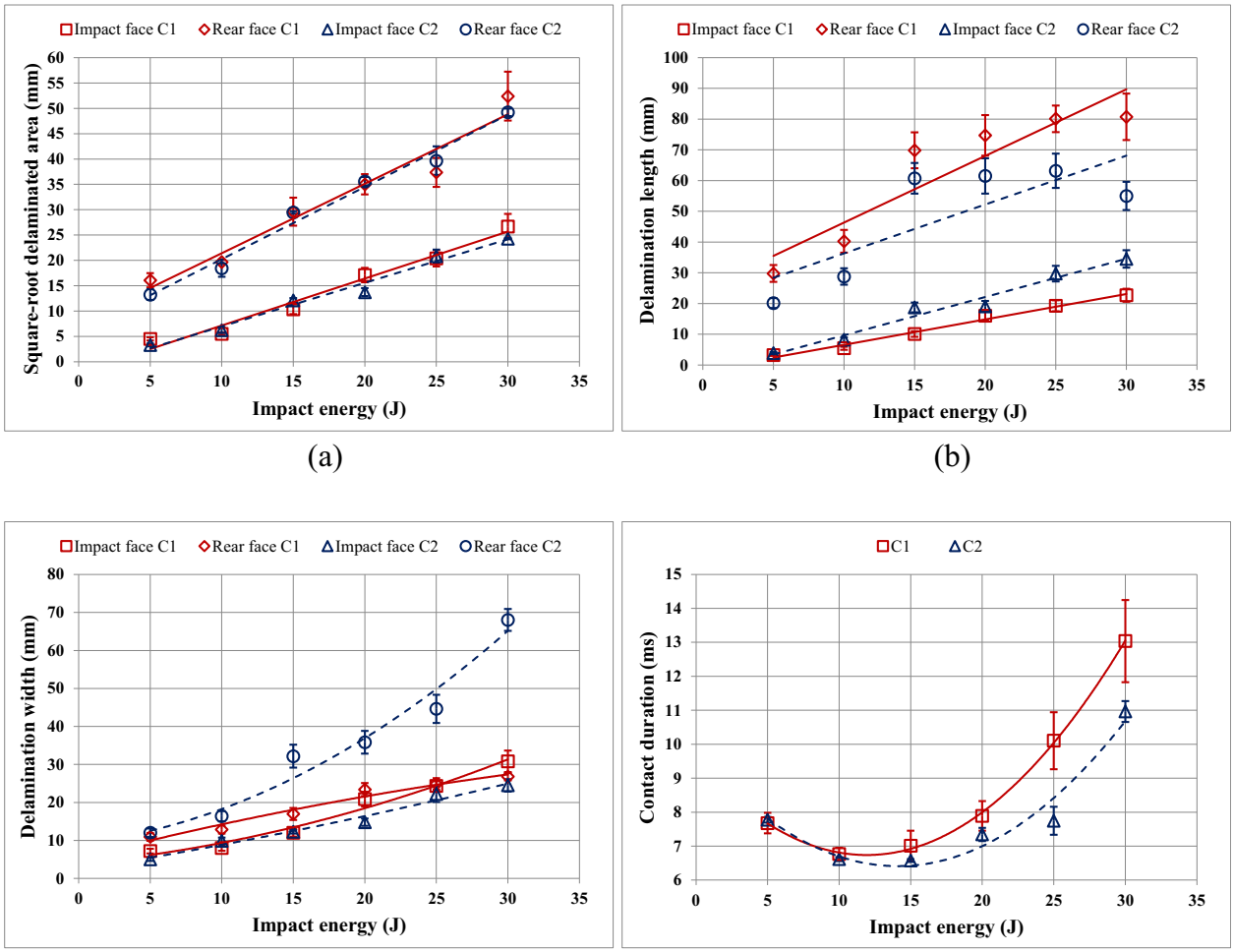

Fig. 10. (a) Square-root delaminated area, (b) delamination length, (c) delamination width and (d) contact duration for composites at various impact energy levels.

4. Discussion

In this section, salient differences in the response of composites due to the separation of composite layers with fibers having the same and different orientations across the composite thickness will be examined. In case of [0/90/90/0] composite, two layers with fibers having 0° orientations are separated by two layers with fibers having 90° orientations. In case of [90/-45/45/0] composite, two layers with fibers having 90° and 0° orientations are separated by two layers with fibers having -45° and 45° orientations. A clear difference is observed between [0/90/90/0] and [90/-45/45/0] composites when considering performance parameters presented in the preceding section. C2 is having a higher first damage force and maximum force to that of C1 at energy levels considered in this study. Similarly, the first cracking energy is higher for C2 and lower for C1. The maximum displacement is higher for C1 and lowers for C2 and so is permanent deformation. The measure of absorbed energy, i.e., damage degree is higher for C1 and lower for C2. C2 outperforms C1 as a measure of impact resistance in terms of having higher levels of first damage and maximum forces, elastic strain energy and bending stiffness. In addition to this, C2 is also having a higher level of first cracking energy along with lower levels of maximum and residual displacements, permanent deformation, and square-root delaminated area.

The observations in Section 3.1 specify that the spread of deformation for composites increases with the level of impact energy. However, at a given level of energy, the spread is affected by the placement of different fiber orientations and is higher for C1 and lower for C2. The two parts of overall deformation occur, local deformation of composite layers due to the crack zone around the site of impact resulting in an impact dent is the first one and deformation of the specimen in the plate or structural mode is the other one. The overall extensional and flexural stiffnesses of the entire composite laminate are responsible for deformation in structural mode. These stiffnesses would be resulted in reducing by delamination between layers as acting of layers will prevail individually and deformation of structure will increase. The observation of the spread of deformation is from images of damaged specimens to which elastic recovery has undergone to a large extent. In case of [0/90/90/0] composite, once delamination takes place, more degradation of overall extensional and flexural stiffnesses are occurred resulting in deformation which is spreading even at lower energy levels. In this case, the behavior of a very small amount of membrane type becomes principal. Once impact energy becomes adequate to cause fiber failure on the rear face with a patch of fiber layer being separated on this face, degradation of local stiffness will occur significantly. This results in deformation around impact site which is more local, rather than scattering the deformation, as observed in case of impact energy levels of 25 J and 30 J (Fig. 4e, f). It should be noted that, once the scattering of deformation reaches to the clamped edge, the response of deformation can be influenced by clamping. However, we rely that the observed response with its overall trend and its dependence on the arrangement of fiber orientation will be the same at least qualitatively. The impact energy also influences the spread of delamination. At lower levels of impact energy, reduction of extensional and flexural stiffnesses will occur through delamination induced by impact causing the spread of deformation as stated before. The separation of composite layers with fibers having the same and different orientations further affects this spread. The extent of delamination increases with increasing levels of impact energy and this will further raise the spread of deformation. However, more concentrated deformation will occur once fiber failure happens with a patch of fiber ply being pushed out on the rear layer at higher levels of energy.

The placement of layers with different fiber orientations affects lateral scatter of delamination and inter-layer opening. This will be evident if images of sectioned samples of Figs. 3, 4, and 5 could be taken. The delamination between layers during the stage when the deformation of composites takes place is mode-II dominated [54]. Therefore, the opening of mode-II delamination takes place further when composites initiate to spring back during the rebound of impactor [55]. Recovery can take place for the composite layer to a large extent, especially at lower levels of impact energy. The extent of relative extensional and flexural stiffnesses of composite layers on either side of delamination will be responsible for the extent of opening up and spreading of delamination during recovery. The values of single and two layers of composites are provided in Table 3. Eqs. (1) and (2) of the classical laminate theory are used to calculate these values as follows

$$A_{ij} = \sum_{k=1}^{n} \left(\overline{Q_{ij}}\right)_k (h_k - h_{k-1}) \tag{1}$$

$$D_{ij} = \frac{1}{3} \sum_{k=1}^{n} \left(\overline{Q_{ij}}\right)_k \left(h_k^3 - h_{k-1}^3\right) \tag{2}$$

where two surfaces of a k^{th} layer (ply) from the mid surface are denoted by distances h_{k-1} and h_k and numbers of layers (plies) and elastic constants of a k^{th} ply are denoted by n and $(\overline{Q_{ij}})_k$[3]. In case of single-layer (like [0]), $h_{k-1} = -t/2$ and $h_k = t/2$, where the thickness is denoted by t.

From Table 3, it can be observed that in case of [0/90/90/0] composite, corresponding extensional and flexural stiffnesses of a single 0° layer along longitudinal direction A_{11} and D_{11} are about 5 times higher to that of adjacent single 90° layer. Also, the corresponding stiffnesses of a single 90° layer along transverse direction A_{22} and D_{22} are about 5 times higher than that of adjacent single 0° layer. Therefore, extent of spread of delamination and opening between [0/90] and [90/0] layers during their recovery will be larger in this case due to higher opening forces exerted between them considering A_{11}, D_{11} and A_{22}, D_{22}, respectively than that of [90/90] layers, in which there is no delamination and interlayer opening. The delamination between [0/90] layers propagates more and less along 0° and 90° fiber directions, respectively considering A_{11} and D_{11}. Whereas, the propagation of delamination between [90/0] layers happens more and less along 90° and 0° fiber directions, respectively considering A_{22} and D_{22}. The corresponding stiffnesses A_{12}, D_{12} and A_{66}, D_{66} of single 0° layer are equal to that of adjacent single 90° layer. There are no components of stiffnesses A_{16}, D_{16} and A_{26}, D_{26} for single 0° layer, single 90° layer and therefore [0/90] laminate.

In case of [90/-45/45/0] composite, it can be observed that corresponding stiffness components A_{11} and D_{11} of single -45° layer are about 2 times higher than that of adjacent single 90° layer. Whereas the corresponding components of stiffnesses A_{22} and D_{22} of a single 90° layer are about 2.4 times higher than that of adjacent single -45° layer. Therefore opening forces exerted between [90/-45] layers during their recovery will be higher resulting in the spread of delamination which is more and larger opening, in this case, considering A_{22}, D_{22} than that of [-45/45] layers in which there is no delamination and interlayer opening. The delamination between [90/-45] layers propagates more and less along 90° and -45° fiber directions, respectively considering A_{22} and D_{22}. Whereas the propagation of delamination between [-45/90] layers happens more and less along -45° and 90° fiber directions, respectively considering A_{11} and D_{11}. The corresponding stiffness components A_{12}, D_{12} and A_{66}, D_{66} of single -45° layer are about 4.2 and 3.5 times higher than that of adjacent single 90° layer, respectively. This leads to higher opening forces exerted between [-45/90] layers during their recovery resulting in more delamination spread and a larger amount of opening considering A_{12}, D_{12} than that of A_{66}, D_{66} and A_{11}, D_{11}. Similarly, corresponding stiffnesses A_{22} and D_{22} of a single 45° layer are about 2 times higher than that of adjacent single 0° layer. Whereas, the corresponding stiffnesses A_{11} and D_{11} of a single 0° layer are about 2.4 times higher than that of adjacent single 45° layer. Therefore opening forces exerted between [45/0] layers during their recovery will be the same as that of [-45/90] layers considering A_{22}, D_{22} and A_{11}, D_{11}, respectively. Also, these [45/0] layers will be having more delamination spread and larger opening during their retrieval considering A_{22}, D_{22} than that of [-45/45] layers in which there is no delamination and interlayer opening. The

Table 3
Stiffness of single and two layers of composites (a) extensional and (b) flexural.

(a)						
Layer	A_{11} (kN/mm)	A_{22} (kN/mm)	A_{12} (kN/mm)	A_{16} (kN/mm)	A_{26} (kN/mm)	A_{66} (kN/mm)
Single 0° layer	15.516	3.226	0.935	0	0	1.192
Single 45° layer	6.346	6.346	3.961	3.072	3.072	4.218
Single 90° layer	3.226	15.516	0.935	0	0	1.192
Single -45° layer	6.346	6.346	3.961	-3.072	-3.072	4.218
[0/90] laminate	18.743	18.743	1.871	0	0	2.385
[90/-45] laminate	9.572	21.862	4.896	-3.072	-3.072	5.410
[45/0] laminate	21.862	9.572	4.896	3.072	3.072	5.410
(b)						
Layer	D_{11} (kN-mm)	D_{22} (kN-mm)	D_{12} (kN-mm)	D_{16} (kN-mm)	D_{26} (kN-mm)	D_{66} (kN-mm)
Single 0° layer	0.323	0.067	0.019	0	0	0.025
Single 45° layer	0.132	0.132	0.082	0.064	0.064	0.088
Single 90° layer	0.067	0.323	0.019	0	0	0.025
Single -45° layer	0.132	0.132	0.082	-0.064	-0.064	0.088
[0/90] laminate	1.562	1.562	0.156	0	0	0.199
[90/-45] laminate	0.798	1.822	0.408	-0.256	-0.256	0.451
[45/0] laminate	1.822	0.798	0.408	0.256	0.256	0.451

delamination between [0/45] layers propagates more and less along 0° and 45° fiber directions, respectively considering A_{11} and D_{11}. Whereas, the propagation of delamination between [45/0] layers happens more and less along 45° and 0° fiber directions, respectively considering A_{22} and D_{22}. The corresponding stiffnesses A_{12}, D_{12} and A_{66}, D_{66} of single 45° layer are about 4.2 and 3.5 times higher than that of adjacent single 0° layer, respectively. This leads to opening forces that are higher exerting between [45/0] layers during their retrieval resulting in more spread of delamination and a larger amount of opening considering A_{12}, D_{12} than that of A_{66}, D_{66} and A_{22}, D_{22}. The ratio of corresponding components of stiffnesses A_{16}, D_{16} and A_{26}, D_{26} for single 90° layer to single -45° layer and that of a single 0° layer to single 45° layer is zero.

It is to be noted that the extent of lateral spread of delamination and opening between [0/90] and [90/0] layers of [0/90/90/0] composite are about 2 times more than that of corresponding [90/-45] and [45/0] layers of [90/-45/45/0] composite during their recovery considering A_{11}, D_{11} and A_{22}, D_{22}, respectively. However, the spreading and opening of delamination between [90/-45] and [45/0] layers of [90/-45/45/0] composite are about 2.6 and 2.3 times more than that of corresponding [0/90] and [90/0] layers of [0/90/90/0] composite during their recovery considering A_{12}, D_{12} and A_{66}, D_{66}, respectively. Delamination between layers enables the behavior of composites with deformation of membrane type of very small amount in contrast to the deformation of the flexural type of a structure that is monolithic and intact. This is because layers are not enormously separated in composites. This separation will be higher for [0/90/90/0] composite compared to that of [90/-45/45/0] composite considering corresponding stiffness components A_{11}, D_{11} and A_{22}, D_{22} as discussed above. The energy during impact is reflected to be more efficiently absorbed by the behavior of membrane type. This is more in case of thinner composites where the large deflection of laminate happens several times higher than the laminate thickness [56, 57, 58]. Therefore, separation of fiber orientation through the thickness, particularly in case of [0/90/90/0] composite, very small amount of membrane type deformation can be enabled more efficiently than that of [90/-45/45/0] composite.

5. Conclusions

The low velocity impact response of two different composites of the same thickness is examined. Fibers with the same and different orientations are used to separate composite layers across the thickness. The parameters used to compare the performance of composites include first damage and maximum forces, first cracking energy, bending stiffness, elastic strain energy, elastic, residual and maximum displacements, permanent deformation, damage degree, square-root delaminated area, delamination length, and contact duration. The following can be concluded from the results of this study.

- [90/-45/45/0] composite is having a higher first damage force and maximum force for a given level of impact energy. The first cracking energy is higher for [90/-45/45/0] composite accumulating lower damage. The resistance to first cracking energy is lower for [0/90/90/0] composite. In case of [90/-45/45/0] composite, the record of force-displacement response is stiffer up to maximum force at all energy levels indicating higher bending stiffness and better impact damage resistance. The elastic strain energy is higher for [90/-45/45/0] composite.
- Elastic displacement corresponding to elastic strain energy is higher for [90/-45/45/0] composite whereas residual displacement corresponding to the energy absorbed is higher for [0/90/90/0] composite. The maximum displacement and permanent deformation are lower when composite layers are having a fiber orientation of [90/-45/45/0].
- The damage degree which is a measure of absorbed energy is higher for [0/90/90/0] composite at all energy levels and is 8 % higher than that of [90/-45/45/0] composite at 5 J impact energy. Whereas the same is 18 %, 3 %, and 4 % higher at 10 J, 15 J, and 25 J impact energy, respectively. Consequently, variance in damage degree between two composites becomes lesser at the level of impact energy at which perforation takes place, i.e., 30 J.
- The opening of delamination between dissimilar layers of composites specifically spread and the extent of the opening is affected by separating composite layers. These parameters are higher for [0/90/90/0] and [90/-45/45/0] composites considering stiffnesses (A_{11}, D_{11}), (A_{22}, D_{22}) and (A_{12}, D_{12}), (A_{66}, D_{66}), respectively.
- The square-root delaminated area and delamination length on the rear face are lower for [90/-45/45/0] composite at all energy levels. In case of [0/90/90/0] composite, an equal amount of peanut shape delamination area has occurred between [0/90] and [90/0] layers with its major axis is oriented along 0° and 90° fiber directions considering stiffnesses (A_{11}, D_{11}) and (A_{22}, D_{22}), respectively. Whereas in case of [90/-45/45/0] composite, equal amount of peanut shape delamination area has occurred between [-45/90] and [45/0] layers with its major axis is oriented along -45° and 45° fiber directions considering stiffnesses (A_{11}, D_{11}), (A_{12}, D_{12}), (A_{66}, D_{66}) and (A_{22}, D_{22}), (A_{12}, D_{12}), (A_{66}, D_{66}), respectively. The contact duration is lower for [90/-45/45/0] composite at all impact energy levels.

Declarations

Author contribution statement

Ankush P. Sharma: Conceived and designed the experiments; Performed the experiments; Analyzed and interpreted the data; Contributed reagents, materials, analysis tools or data; Wrote the paper.

Sanan H. Khan: Conceived and designed the experiments; Performed the experiments; Wrote the paper.

R. Velmurugan: Analyzed and interpreted the data; Contributed reagents, materials, analysis tools or data; Wrote the paper.

Funding statement

This research did not receive any specific grant from funding agencies in the public, commercial, or not-for-profit sectors.

Competing interest statement

The authors declare no conflict of interest.

Additional information

No additional information is available for this paper.

Acknowledgements

The authors conducted the experiments in Advanced Material Characterization Laboratory, Department of Aerospace Engineering, Indian Institute of Technology Kanpur, Kanpur, India.

References

[1] E. Sevkat, B. Liaw, F. Delale, B.B. Raju, Drop-weight impact of plain-woven hybrid glass–graphite/toughened epoxy composites, Compos. Appl. Sci. Manuf. 40 (8) (2009) 1090–1110.
[2] A. Azzam, W. Li, Experimental investigation on the impact behaviour of composite laminate, Fibres Text. East. Eur. 23 (1(109)) (2015) 77–84.
[3] R.M. Jones, Mechanics of Composite Materials, second ed., Taylor and Francis, New York, 1999.
[4] R.W. Rydin, A. Locurcio, V.M. Karbhari, Influence of reinforcing layer orientation on impact response of plain weave RTM composites, J. Reinf. Plast. Compos. 14 (11) (1995) 1199–1225.
[5] E. Wu, L.-C. Chang, Loading rate effect on woven glass laminated plates by penetration force, J. Compos. Mater. 32 (8) (1998) 702–721.
[6] M. Wisheart, M.O.W. Richardson, Low velocity response of simple geometry pultruded glass/polyester composite, J. Mater. Sci. 34 (2) (1999) 395–406.
[7] H.Y. Choi, H.S. Wang, F.-K. Chang, Effect of laminate configuration and impactor's mass on the initial impact damage of graphite/epoxy composite plates due to line-loading impact, J. Compos. Mater. 26 (6) (1992) 804–827.
[8] A. Kessler, A.K. Bledzki, Low velocity impact behavior of glass/epoxy cross-ply laminates with different fiber treatments, Polym. Compos. 20 (2) (1999) 269–278.
[9] G.A. Schoeppner, S. Abrate, Delamination threshold loads for low velocity impact on composite laminates, Compos. Appl. Sci. Manuf. 31 (9) (2000) 903–915.
[10] G. Belingardi, R. Vadori, Low velocity impact tests of laminate glass-fiber-epoxy matrix composite material plates, Int. J. Impact Eng. 27 (2) (2002) 213–229.
[11] T. Gómez-del Río, R. Zaera, E. Barbero, C. Navarro, Damage in CFRPs due to low velocity impact at low temperature, Compos. B Eng. 36 (1) (2005) 41–50.
[12] R. Hosseinzadeh, M.M. Shokrieh, L. Lessard, Damage behavior of fiber reinforced composite plates subjected to drop weight impacts, Compos. Sci. Technol. 66 (1) (2006) 61–68.
[13] T. Mitrevski, I.H. Marshall, R. Thomson, The influence of impactor shape on the damage to composite laminates, Compos. Struct. 76 (1–2) (2006) 116–122.
[14] M.G. Babu, R. Velmurugan, N.K. Gupta, Energy absorption capability of thin laminates subjected to heavy-mass projectile impact of varying nose geometries, Int. J. Crashworthiness 13 (3) (2008) 237–246.
[15] M. Aktaş, C. Atas, B.M. İçten, R. Karakuzu, An experimental investigation of the impact response of composite laminates, Compos. Struct. 87 (4) (2009) 307–313.
[16] B.M. Icten, C. Atas, M. Aktas, R. Karakuzu, Low temperature effect on impact response of quasi-isotropic glass/epoxy laminated plates, Compos. Struct. 91 (3) (2009) 318–323.
[17] M. Sayer, N.B. Bektas, O. Sayman, An experimental investigation on the impact behavior of hybrid composite plates, Compos. Struct. 92 (5) (2010) 1256–1262.
[18] R. Karakuzu, E. Erbil, M. Aktas, Impact characterization of glass/epoxy composite plates: an experimental and numerical study, Compos Part B 41 (5) (2010) 388–395.
[19] C. Akin, M. Senel, An experimental study of low velocity impact response for composite laminated plates, in: Proceedings of Fen Bilimleri Enstitusu Dergisi, Nisan, 2010. ISSN-1302-3055.
[20] C. Evci, M. Gülgeç, An experimental investigation on the impact response of composite materials, Int. J. Impact Eng. 43 (2012) 40–51.
[21] E.M. Soliman, M.P. Sheyka, M.R. Taha, Low-velocity impact of thin woven carbon fabric composites incorporating multi-walled carbon nanotubes, Int. J. Impact Eng. 47 (2012) 39–47.
[22] M. Quaresimin, M. Ricotta, L. Martello, S. Mian, Energy absorption in composite laminates under impact loading, Composites Part B 44 (1) (2013) 133–140.
[23] M. Meo, F. Marulo, M. Guida, S. Russo, Shape memory alloy hybrid composites for improved impact properties for aeronautical applications, Compos. Struct. 95 (2013) 756–766.
[24] M. Rahman, M. Hosur, S. Zainuddin, U. Vaidya, A. Tauhid, A. Kumar, J. Trovillion, S. Jeelani, Effects of amino-functionalized MWCNTs on ballistic impact performance of E-glass/epoxy composites using a spherical projectile, Int. J. Impact Eng. 57 (2013) 108–118.
[25] D. Zhang, Y. Sun, L. Chen, N. Pan, A comparative study on low-velocity impact response of fabric composite laminates, Mater. Des. 50 (2013) 750–756.
[26] I. Taraghi, A. Fereidon, F. Taheri-Behrooz, Low-velocity impact response of woven Kevlar/epoxy laminated composite reinforced with multi-walled carbon nanotubes at ambient and low temperature, Mater. Des. 53 (2014) 152–158.
[27] S. Agarwal, K.K. Singh, P.K. Sarkar, Impact damage on fiber-reinforced polymer matrix Composite- A review, J. Compos. Mater. 48 (3) (2014) 317–332.
[28] K.K. Namala, P. Mahajan, N. Bhatnagar, Digital image correlation of low- velocity impact on a glass/epoxy composite, Int. J. Comput. Methods Eng. Sci. Mech. 15 (3) (2014) 203–217.
[29] F. Sarasini, J. Tirillò, L. Ferrante, M. Valente, T. Valente, L. Lampani, P. Gaudenzi, S. Cioffi, S. Iannace, L. Sorrentino, Drop-weight impact behaviour of woven hybrid basalt–carbon/epoxy composites, Composites Part B 59 (2014) 204–220.
[30] R.S. Sikarwar, R. Velmurugan, N.K. Gupta, Influence of fiber orientation and thickness on the response of glass/epoxy composites subjected to impact loading, Compos. B Eng. 60 (2014) 627–636.
[31] G. Balaganesan, R. Velmurugan, M. Srinivasan, N.K. Gupta, K. Kanny, Energy absorption and ballistic limit of nanocomposite laminates subjected to impact loading, Int. J. Impact Eng. 74 (2014) 57–66.
[32] R. Reghunath, M. Lakshmanan, K.M. Mini, Low velocity impact analysis on glass fiber reinforced composites with varied volume fractions, IOP Conf. Ser. Mater. Sci. Eng. 73 (2015).
[33] N.K. Singh, K.K. Singh, Review on impact analysis of FRP composite validated by LS-DYNA, Polym. Compos. 36 (2015) 1786–1798.
[34] C. Evci, Thickness-dependent energy dissipation characteristics of laminated composites subjected to low velocity impact, Compos. Struct. 133 (2015) 508–521.
[35] K.K. Singh, N.K. Singh, R. Jha, Analysis of symmetric and asymmetric glass fiber reinforced plastic laminates subjected to low-velocity impact, J. Compos. Mater. 50 (14) (2016).
[36] A.K. Bandaru, V.V. Chavan, S. Ahmad, R. Alagirusamy, N. Bhatnagar, Low velocity impact response of 2D and 3D Kevlar/polypropylene composites, Int. J. Impact Eng. 93 (–) (2016) 136–143.
[37] N.K. Singh, P. Rawat, K.K. Singh, Impact response of quasi- isotropic asymmetric carbon fabric/epoxy laminate infused with MWCNTs, Advances in Materials Science and Engineering 7 (2016), 7541468.
[38] A.K. Bandaru, S. Patel, Y. Sachan, R. Alagirusamy, N. Bhatnagar, S. Ahmad, Low velocity impact response of 3D angle-interlock Kevlar/basalt reinforced polypropylene composites, Mater. Des. 105 (2016) 323–332.
[39] M.K. Hazzard, S. Hallett, P.T. Curtis, L. Lannucci, R.S. Trask, Effect of fibre orientation on the low velocity impact response of thin Dyneema® composite laminates, Int. J. Impact Eng. 100 (2017) 35–45.
[40] R.S. Sikarwar, R. Velmurugan, N.K. Gupta, Effect of Velocity and fibres on impact performance of composite laminates-Analytical and experimental approach, Int. J. Crashworthiness 22 (6) (2017).
[41] M. Truong, W. Zhong, S. Boyko, M. Alcock, A comparative study on natural fibre density measurement, J. Text. Inst. 100 (6) (2009) 525–529.
[42] S.H. Khan, A.P. Sharma, Progressive damage modeling and interface delamination of cross-ply laminates subjected to low velocity impact, J. Strain Anal. Eng. Des. 53 (6) (2018) 435–445.
[43] ASTM D5628-10, Standard Test Method for Impact Resistance of Flat, Rigid Plastic Specimens by Means of a Falling Dart (Tup or Falling Mass), ASTM International, West Conshohocken, PA, 2010.
[44] G.A.O. Davies, X. Zhang, Impact damage prediction in carbon composite structures, Int. J. Impact Eng. 16 (1) (1995) 149–170.
[45] L. Greszczuk (Ed.), Foreign Object Impact Damage to Composites, ASTM International, West Conshohocken, PA, 1975.
[46] S.H. Khan, A.P. Sharma, V. Parameswaran, An Impact induced damage in composite laminates with intra-layer and inter-laminate damage, Procedia Engineering 173 (2017) 409–416.
[47] H.-Y.T. Wu, G.S. Springer, Measurements of matrix cracking and delamination caused by impact on composite plates, J. Compos. Mater. 22 (6) (1988) 518–532.
[48] D. Liu, Impact-induced delamination—a view of bending stiffness mismatching, J. Compos. Mater. 22 (7) (1988) 674–692.
[49] C. Atas, An experimental investigation on the impact response of fiberglass/aluminum composites, J. Reinf. Plast. Compos. 26 (14) (2007) 1479–1491.
[50] M. Sadighi, T. Pärnänen, R.C. Alderliesten, M. Sayeaftabi, R. Benedictus, Experimental and numerical investigation of metal type and thickness effects on the impact resistance of fiber metal laminates, Appl. Compos. Mater. 19 (3–4) (2012) 545–559.
[51] D. Liu, B.B. Raju, X. Dang, Size effects on impact response of composite laminates, Int. J. Impact Eng. 21 (10) (1998) 837–854.
[52] C. Atas, O. Sayman, An overall view on impact response of woven fabric composite plates, Compos. Struct. 82 (3) (2008) 336–345.
[53] S. Zhu, G.B. Chai, Low-velocity impact response of fiber-metal laminates – a theoretical approach, Proc. Inst. Mech. Eng. L J. Mater. Des. Appl. 228 (4) (2014) 301–311.

[54] G. Caprino, V. Lopresto, C. Scarponi, G. Briotti, Influence of material thickness on the response of carbon-fabric/epoxy panels to low velocity impact, Compos. Sci. Technol. 59 (15) (1999) 2279–2286.
[55] T. Pärnänen, M. Kanerva, E. Sarlin, O. Saarela, Debonding and impact damage instainless steel fibre metal laminates prior to metal fracture, Compos. Struct. 119 (2015) 777–786.
[56] A. Vlot, M. Krull, Impact damage resistance of various fibre metal laminates, Le J.de Physique IV 07 (1997). C3–1045–C3–1050.
[57] H. Ahmadi, G.H. Liaghat, H. Sabouri, E. Bidkhouri, Investigation on the high velocity impact properties of glass-reinforced fiber metal laminates, J. Compos. Mater. 47 (13) (2013) 1605–1615.
[58] H. Dabiryan, F. Hasanalizade, M. Sadighi, Low-velocity impact behavior of composites reinforced with weft-knitted spacer glass fabrics, J. Ind. Text. 49 (4) (2019).